Journal of Physical Science and Application 4 (7) (2014) 403-411

Laser Doppler Measurements of Twin Impinging Jets Aligned with a Crossflow

Jorge M.M. Barata[1], Pedro S.D. Carvalho[1], Fernando M.S.P. Neves[1], André R.R. Silva[1], Diana F.C. Vieira[1] and Diamantino F.G. Durão[2]

1. Departmentof Aerospace Sciences, University of Beira Interior, Covilhã 6200-001, Portugal

2. Instituto Lusíada de Investigação e Desenvolvimento, Universidade Lusíada, Lisbon 1349-001, Portugal

Received: April 25, 2014 / Accepted: June 13, 2014 / Published: July 15, 2014.

Abstract: This paper presents a detailed analysis of the complex flow beneath two impinging jets aligned with a low-velocity crossflow which is relevant for the future F-35 VSTOL configuration, and provides a quantitative picture of the main features of interest for impingement type of flows. The experiments were carried out for a Reynolds number based on the jet exit conditions of $Re_j = 4.3 \times 10^4$, an impingement height of 20.1 jet diameters and for a velocity ratio between the jet exit and the crossflow $V_R = V_j/U_o$ of 22.5. The rear jet is located at $S = 6\ D$ downstream of the first jet. The results show a large penetration of the first (upstream) jet that is deflected by the crossflow and impinges on the ground, giving rise to a ground vortex due to the collision of the radial wall and the crossflow that wraps around the impinging point like a scarf. The rear jet (located downstream) it is not so affected by the crossflow in terms of deflection, but due to the downstream wall jet that flows radially from the impinging point of the first jet it does not reach the ground. The results indicate a new flow pattern not yet reported so far, that for a VSTOL aircraft operating in ground vicinity with front wind or small forward movement may result in enhanced under pressures in the aft part of the aircraft causing a suction down force and a change of the pitching moment towards the ground.

Key words: VSTOL, ground vortex, turbulence, complex flows.

Nomenclatures

D:	Diameter of the jet
H:	Impinging height
K:	Turbulent kinetic energy
Re:	Reynolds number
S:	Spacing of the jets axis in the wind direction
U:	Horizontal velocity, $\overline{U} + u'$
V:	Vertical velocity, $\overline{V} + v'$
W:	Transverse $\overline{W} + w'$
X:	Horizontal coordinate
Y:	Vertical coordinate
Z:	Transverse coordinate

Subscripts

J:	Jet-exit value
O:	Crossflow value

Corresponding author: Jorge M.M. Barata, full professor, hab., PhD, research fields: aerodynamics, computational fluid dynamics and VSTOL. E-mail: jbarata@ubi.pt.

1. Introduction

Turbulent jets impinging on flat surfaces through a low-velocity crossflow are typical in impinging cooling applications in industry [1] as well as of the flow beneath a short/vertical take-off aircraft which is lifting off or landing with zero or small forward momentum [2]. Ground effect may occur and change the lift forces on the aircraft, cause reingestion of exhaust gases into the engine intake and raise fuselage skin temperatures. In this latter application the impingement of each downward-directed jet on the ground results in the formation of a wall jet which flows radially from the impinging point along the ground surface. The interaction of this wall jet with the free stream results in the formation of a ground vortex far upstream of the impinging jet, which has profound implications on the aircraft design. In addition the

collision of the wall jets originates a fountain upwash flow, affecting the forces and moments induced in the aircraft when operating in ground effect. Improved knowledge of impinging flows is therefore necessary to avoid these effects and to be able to model a range of jet-impingement type of applications with practical interest.

Earlier published work has been concentrated on 1, 2, and 3 jets configurations relevant to the Harrier/AV-8B aircraft [2]. In this case, when the aircraft is operating with small forward movement the configuration of interest is 2 impinging jets with the direction of the crossflow perpendicular to the line containing their centers, because each impinging jet is located on the sides of the fuselage.

If attention is concentrated on the next generation of VSTOL aircrafts (X-35/F-35/JSF-Joint Strike Fighter) then no relevant studies can be found, because the impinging jets are aligned with the crossflow, and this geometry has not been considered. In this case a vertically oriented lift fan (SDLF) generates a column of cool air that produces nearly 20,000 pounds of lifting power, along with an equivalent amount of thrust from the vectored rear exhaust (3BSM-Three Bearing Swivel Module). The lift system was successfully demonstrated during a flight testing of the X-35B during the summer of 2001. The complexity of the new VSTOL configuration together with the very stringent requirements has required an enormous amount of R&D in the last decade. On 12th May 2012 the 200th test flight of the F-35B (BF-3) measured stresses on the aircraft during supersonic maneuvers. So, most of the published work reported so far has therefore only peripheral relevance to the F35-B/JSF ground effect problem.

Ref. [3] reports a study of multijet impinging configurations producing upwash fountain flows, which are the heart of the complicated effects by VSTOL aircraft when they operate in ground proximity, but as far as twin jets are concerned only the geometry with the jets side by side was considered. This paper presents a detailed analysis of the complex flow field beneath two impinging jets aligned with a low-velocity crossflow relevant for the new F-35 VSTOL configuration, and provides a quantitative picture of the main features of interest of impingement type of flows.

The remainder of this paper is presented in four sections. Section 2 describes the experimental configuration and measurement procedure, gives details of the laser-Doppler velocimeter and provides assessments of accuracy. The arguments associated with these assessments are based on previous experiments and are presented in condensed form. Section 3 presents the experimental results obtained in the vertical plane of symmetry containing the axis of both jets and quantifies the mean and turbulent velocity characteristics of the flow. The final section summarizes the main findings and conclusions of this work.

2. Experiments

The wind tunnel facility designed and constructed for the present work is schematically shown in Fig. 1. A fan with 15 kW nominal power drives a maximum flow of 3,000 m^3/h through the boundary layer wind tunnel of 300 × 302 mm exit section. Each jet unit of 15 mm inner diameter is mounted vertically in the top of the test section with the axis contained in the vertical plane o symmetry parallel to the crossflow.

The origin of the horizontal, X, and vertical, Y, coordinates is taken at the midpoint between the centers of the jets exit. The X coordinate is positive in the direction of the wind tunnel exit and Y is positive upwards.

The present results were obtained at the vertical plane of symmetry for jet mean velocities of V_j = 36 m/s and mean crossflow velocity of U_0 = 1.6 m/s, corresponding to a velocity ratio, $V_R = V_j/U_o$ of 22.5. The rear jet is located at S = 6D downstream of the first jet (Fig. 2).

The velocity field was measured with a two-color (two-component) Laser-Doppler velocimeter (Dantec

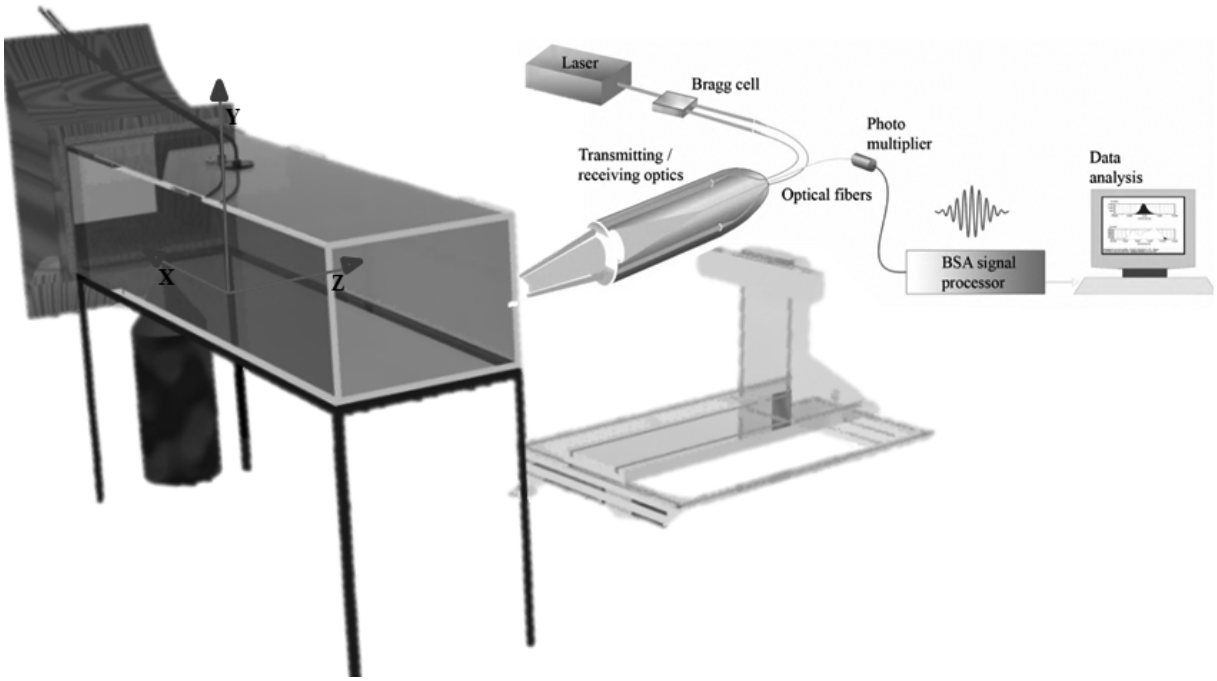

Fig. 1 Experimental set-up.

Table 1 Principal characteristics of the 2D Laser-Doppler velocimeter.

	He-Ne laser	Diode Laser
Wave length, λ (nm)	633	532
Focal length of focusing lens, f (mm)	400	400
Beam diameter at e-2 intensity (mm)	1.35	1.35
Beam spacing, s (mm)	38.87	39.13
Calculated half-angle of beam intersection, θ	2.78°	2.8°
Fringe spacing, δ_f (μm)	6.53	5.45
Velocimeter transfer constant, K (MHz/ms^{-1})	0.153	0.183

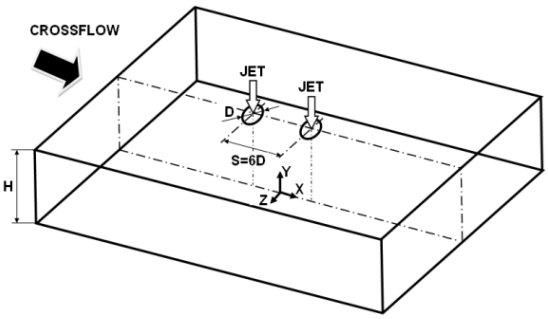

Fig. 2 Geometrical arrangement of the jets.

Flowlite 2D), which comprised a 10 mW He-Ne and a 25 mW diode-pumped frequency doubled Nd:YAG lasers, sensitivity to the flow direction provided by frequency shifting from a Bragg cell at f_0 = 40 MHz, a transmission and backward-scattered light collection focal lens of 400 mm. The half-angle between the beams was 2.8° and the calculated dimensions of the axis of the measuring ellipsoid volume at the e^{-2} intensity locations were 135 × 6.54 × 6.53 μm and 112 × 5.46 × 5.45 μm, respectively (Table 1 for details). The horizontal, *U*, and vertical *V*, mean and turbulent velocities were determined by a two-velocity channel Dantec BSA F60 processor. The seeding of the flow with glycerinparticles of 0.1-5 μm was produced by a smoke generator. The transmitting and collecting optics is mounted on a three-dimensional traversing unit, allowing the positioning of the center of the control volume within ±0.1 mm.

In order to measure the vertical components in near wall regions, the transmitting optics were inclined by half angle of beam intersection and the scattered light

was collected off-axis. Measurements could then be obtained up to 0.5 mm from the ground plate without a significant deterioration of the Doppler signals. Results obtained 20 mm above the ground plate with both the on-axis and the off-axis arrangements have shown a close agreement, within the precision of the equipment.

Errors incurred in the measurement of velocity by displacement and distortion of the measuring volume due to refraction on the duct walls and change in the refractive index were found to be negligibly small and within the accuracy of the measuring equipment. Non-turbulent Doppler broadening errors due to gradients of mean velocity across the measuring volume may affect essentially the variance of the velocity fluctuations [4], but for the present experimental conditions are of the order of $10^{-4}V_j^2$ and, therefore, sufficiently small for their effect to be neglected. The largest statistical (random) errors derived from populations of, at least, 10,000 velocity values were of 0.5% and 3%, respectively for the mean and the variance values, according to the analysis recommended by Yanta and Smith [5] for a 95% confidence interval. No corrections were made for sampling bias, but no correlations were found between Doppler frequencies and time interval between consecutive bursts even in the zones of the flow characterized by the lowest particle arrival rates, suggesting that those effects are unimportant for the present flow conditions.

Systematic errors incurred in the measurements of Reynolds shear stresses can arise from lack of accuracy in the orientation angle on the normal to the anemometer fringe pattern, and can be particularly large in the vicinity of the zones characterized by zero shear stress [6]: for the present experimental conditions the largest errors are expected to be smaller than -2.5%.

3. Results

In this chapter, experimental data obtained are presented and discussed under two headings. First, flow visualization is presented, and then mean and turbulent velocity profiles are presented and discussed for the velocity ratios V_R of 22.5.

3.1 Visualization

Flow visualization was performed using digital direct photography to guide the choice of the measurement locations and to provide a qualitative picture of the flow. The longitudinal vertical plane of symmetry was illuminated with a sheet of light. The photos were taken perpendicular to the vertical plane of symmetry. For all the flows studied, the results have shown (for each jet) a pattern similar to that of a single impinging jet. Fig. 3 identifies the flow development along the vertical plane of symmetry, i.e., $Z = 0$. Each jet has an initial potential-core jet region, where the flow characteristics are identical to those of a free jet, and near the horizontal plate the impingement region, characterized by considerable deflection of the jet. The selected picture shows the wall jet corresponding to the upstream impinging jet which is almost parallel to the ground plate and exhibits behavior similar to that of a radial wall jet where the upstream effects of interaction due to impingement are no longer important. The upstream wall jet interacts with the crossflow and forms a horseshoe vortex close to the ground plate, which wraps around both impinging jets. As a result, two streamwise counter-rotating vortices develop side-to-side and decay further downstream of each impinging zone forming a ground vortex. The nature of each ground vortex is similar to the horseshoe structure known to be generated by the deflection of a boundary layer by a solid obstacle [7], but is different from the vortex pair known to exist in a “bent-over” jet in a crossflow far from the ground [8]. No evidence of a ground vortex corresponding to the downstream impinging jet could be confirmed, which is an indication that the upstream impinging jet and its ground vortex are blocking the crossflow and provoking an alteration to the flow pattern. If the jets were positioned side by side in front of the crossflow two ground vortexes would appear as well as a fountain

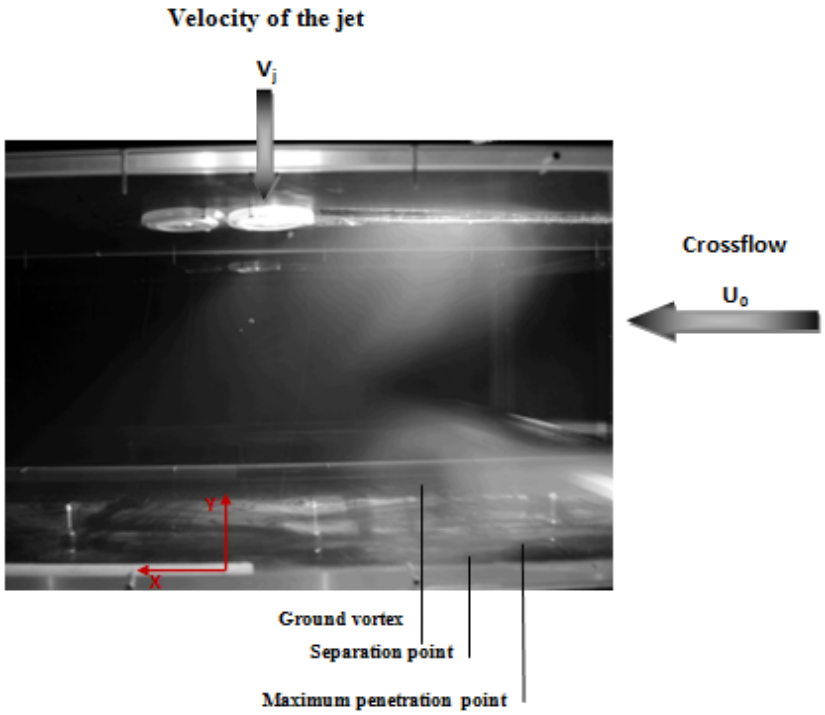

Fig. 3 Visualization of the twin jet flow in the vertical plane of symmetry for $Re_j = 4.3 \times 10^4$, $V_j/U_o = 22.5$, $H/D = 20.1$, and $S/D = 6$.

flow in the vertical plane of symmetry due to the collision of the two individual radial wall jets [9-10]. In the present case for a velocity ratio between the jet and the crossflow of $V_R = 22.5$ no fountain flow could be detected.

Analysis of Fig. 3 also suggests that the crossflow is deflected sideways by the penetration of the jet and may cause a recirculation region just downstream of the discharge, away from the ground plate, but cannot be clearly identified. These features of the flow are quantified in Figs. 4-6 through a detailed set of mean and turbulent velocity measurements obtained in the vertical plane of symmetry ($Z = 0$) for a Reynolds number based on the jet-exit conditions of 4.3×10^4, a free stream to jet velocity ratio, $V_R = V_j/U_o$ of 22.5, a jet height to jet diameter ratio, H/D, of 20.1, and a spacing between the jets in the wind direction, S/D, of 6.

3.2 Measurements

Fig. 4 shows vertical profiles of the mean horizontal velocity component, $\overline{U}$, along the vertical plane of symmetry ($Z = 0$).

The mean horizontal velocity profiles at X/D = -2.93, -1.47, 0 and +1.47 show negative values near the ground ($Y = 0$) that correspond to the upstream wall jet, revealing that the first impinging jet was deflected by the crossflow. The impinging point of the first jet is located at about X/D = +2.93 in a position that is vertically near the axis of the rear jet exit (X/D = +3), which is more strongly deflected due to this interference. As a consequence, the downstream wall jet of the first jet and the rear jet seems to merge rapidly in a single flow in the crossflow direction. These profiles exhibit maximum positive (downstream) values of the mean horizontal velocity component between Y = 100 mm and 150 mm that reach twice the crossflow velocity. This means that no upstream wall jet resulting from the rear jet exists, but the complete jet is deflected by the crossflow. This result is consistent with the conclusions of Ref. 4 that found for a single impinging jet flow that the ground vortex blocks the passage of the confined crossflow increasing the velocity of the crossflow that passes over. So, for this configuration the final result is that the rear jet "feels" a

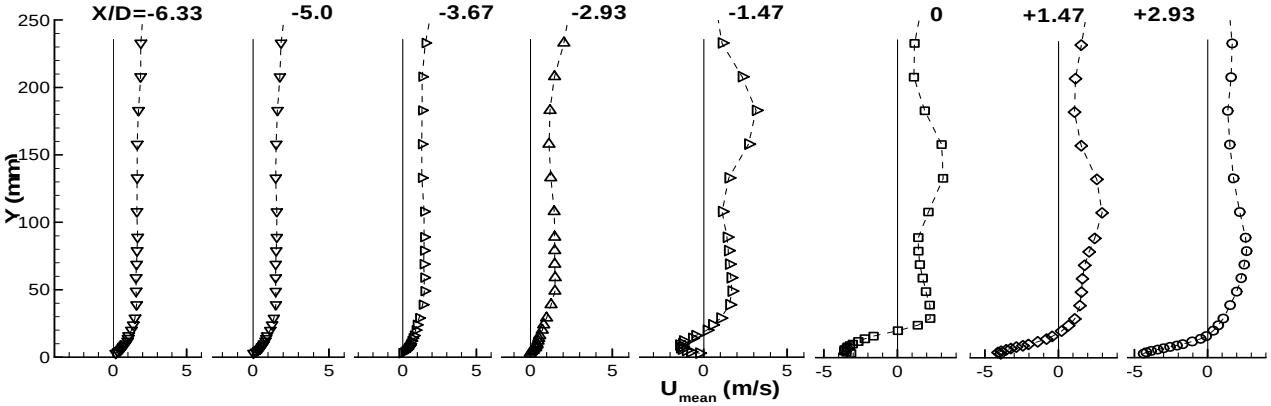

Fig. 4 Vertical profiles of the mean horizontal velocity component, $\bar{U}$, along the longitudinal (symmetry) plane crossing the center of the twin jets. $Re_j = 4.3 \times 10^4$, $V_j/U_o = 22.5$, $H/D = 20.1$, and $S/D = 6$.

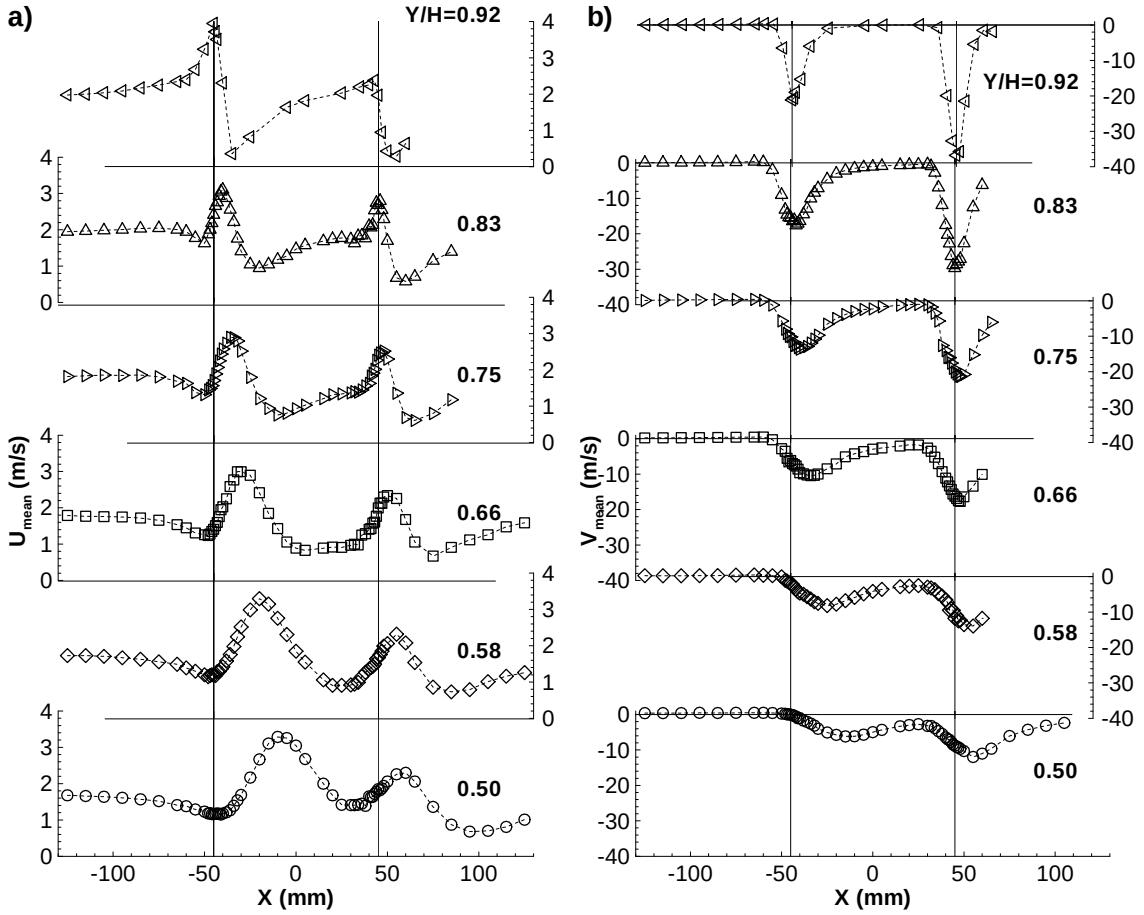

Fig. 5 Horizontal profiles of the mean velocity characteristics along the longitudinal (symmetry) plane crossing the center of the twin jets. $Re_j = 4.3 \times 10^4$, $V_j/U_o = 22.5$, $H/D = 20.1$, and $S/D = 6$. (a) Horizontal velocity, $\bar{U}$. (b) Vertical velocity, $\bar{V}$.

smaller jet-to-crossflow velocity ratio and no impingement occurs. In the practical situation of a VSTOL aircraft this may result in a different pressure distribution in the under surface of the aircraft, that with front wind or small forward movement may result in enhanced under pressures in the aft part of the aircraft causing a suction down force and a change of the pitching moment towards the ground.

Figs. 5a and 5b show horizontal profiles of horizontal, $\bar{U}$, and vertical, $\bar{V}$, mean velocity

components, quantify the development of the impinging jets and confirm the above description of the flow. The measurements, and particularly those of the vertical velocity component, do not identify a centrally located fountain rising from the ground plate without interference from the main jets, as it occurs in practical VSTOL applications [10].

This result confirms our hypothesis that the alignment of the twin jets with the crossflow would create a special flow pattern not yet reported before. The wall jet resulting from the first jet flows underneath the rear one, but the ground vortex formed upstream is only interfering away from the vertical symmetry plane.

The mean vertical velocity component is always positive from the upper wall (Y/H = 1) up to the middle of the crossflow (Y/H = 0.5), confirming the conclusions drawn from the vertical velocity profiles in the lower part of the crossflow and discussed in the previous paragraphs.

The asymmetry of the flow can be confirmed from the horizontal profiles of the mean vertical velocity component with higher peaks up to 10% of the vertical velocity in the upstream side (X < -50 mm or 3.33 D). The middle value between the maximum and the minimum of the mean horizontal velocity component or the mean vertical velocity components can be used to indicate the center of the jet, and in the upstream side it moves in the crossflow direction from -43.02 mm at Y/H = 0.92 to 10.47 mm at Y/H = 0.5 corresponding to a deflection angle of 21.9º. The downstream jet is protected from the action of the crossflow by the first

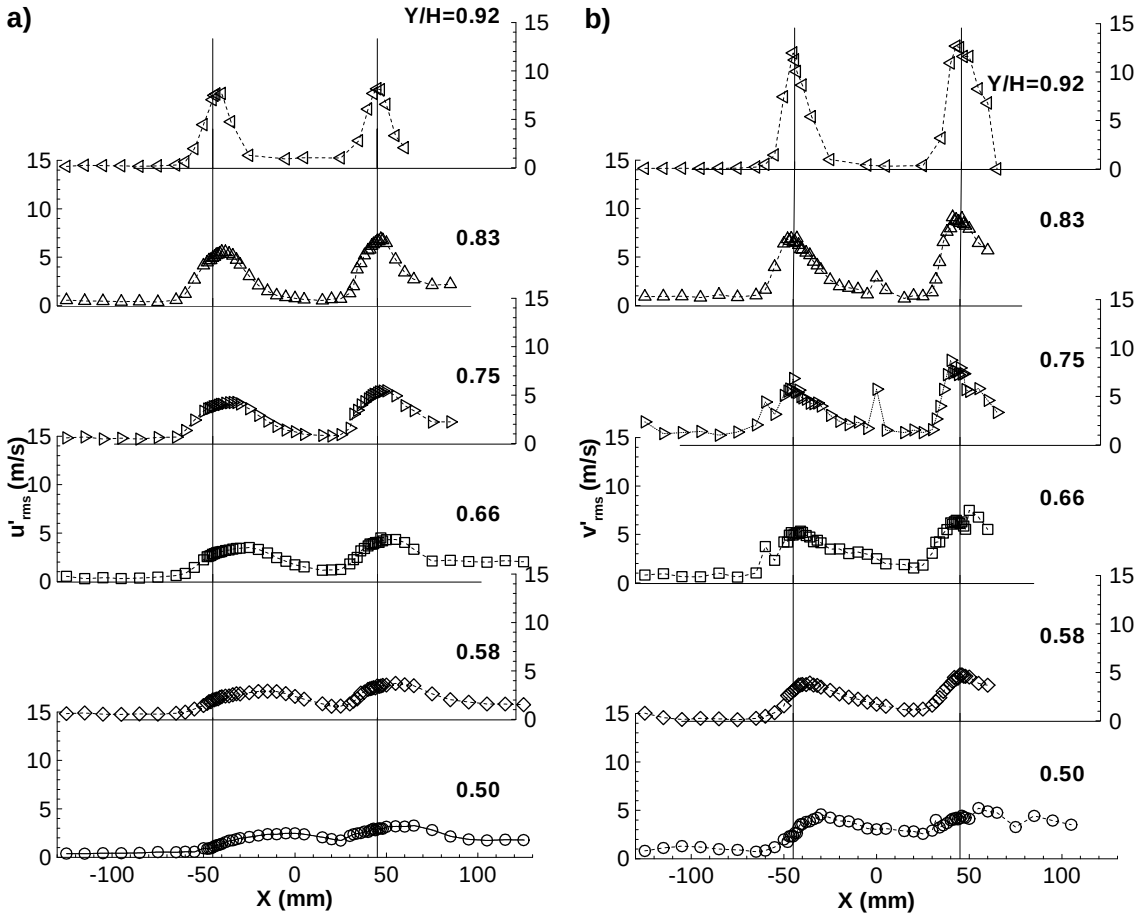

Fig. 6 Horizontal profiles of the fluctuating velocity characteristics along the longitudinal (symmetry) plane crossing the center of the twin jets. Re_j = 4.3 × 10^4, V_j/U_o = 22.5, H/D = 20.1, and S/D = 6. (a) Horizontal rms velocity, $\sqrt{\overline{u'^2}}$. (b) Vertical rms velocity, $\sqrt{\overline{v'^2}}$.

jet and as a consequence it is less deflected: the center of the jet is almost coincident with the geometrical axis of the exit, and for $Y/H = 0.5$ it is located at $X/D = +4.0$ corresponding to an inclination angle of 12.3º. However, considering the maximum of the mean vertical velocity component the calculated inclination angle is only 4.8º, which reinforces the conclusion, and the difference is probably associated with an enhanced entrainment of the rear jet due to its smaller angle with the surrounding flow.

Fig. 6 shows horizontal profiles of the normal stresses, $\overline{u'^2}$ and $\overline{v'^2}$, in a *rms* form, and show results that are somewhat surprising at first sight, because it seems that it is not possible to identify completely the shear layer surrounding the impinging jets for the highest stations ($Y/H = 0.92$ and 0.83). However, it should be noted that the diameter of the jet is only 15 mm and so the peak observed corresponds to the shear layer which exhibits similar values in the upstream and downstream sides of the jet.

The peaks in the fluctuating vertical velocity components occur in the upstream side of the first jet as expected, because in this region the higher velocity gradients occur. Other peaks were observed near $X = 0$ for the $X/H = 0.83$ and 0.75 profiles that correspond to the downstream side of the first impinging jet. For the $X/H = 0.66$ profile the peak is very weak, and for the lower profiles they cannot be pointedly identified, confirming the rapid mixing between the jets as already detected from the lower part of the flow through the vertical velocity profiles. For the second (downstream) impinging jet the shear layer surrounding the jet cannot be clearly identified. However, for the $Y/H = 0.66$ profile a small decrease in the normal vertical stress is noted near the center of the jet, but the peaks around the jet are so close that the minimum value is somewhat masked.

4. Conclusions

A laser Doppler velocimeter was used to provide information on the flowfield created by twin impinging jets aligned with a low velocity crossflow. The experiments were carried out for a Reynolds number based on the jet exit conditions of $Re_j = 4.3 \times 10^4$, an impingement height of 20.1 jet diameters and for a velocity ratio between the jet exit and the crossflow $V_R = V_j/U_o$ of 22.5. The rear jet is located at $S = 6\ D$ downstream of the first jet.

The results show a large penetration of the first (upstream) jet, which is deflected by the crossflow and impinges on the ground, giving rise to a ground vortex due to the collision of the radial wall and the crossflow that wraps around the impinging point like a scarf. The rear jet is not so affected by the crossflow in terms of deflection because it is protected by the upstream jet, but due to the downstream wall jet that flows radially from the impinging point the first jet does not reach the ground. Also, due to the confinement and the ground vortex, the crossflow is blocked and accelerates in the upper part and also contributes to an enhanced mixing of each secondary flow. As consequence, no upstream wall jet or ground vortex resulting from the second (downstream) jet was detected. The result of the rear jet impinging on the downstream wall jet resulting from the first jet had not been reported so far and requires further investigation.

The shear layers surrounding the jet cannot be clearly identified from the fluctuating velocities that do not exhibit distinct peaks in the edges, and the values in the center are also high. Nevertheless, the high levels of turbulent velocities correspond to the expected values in the upstream and downstream sides of the impinging jets.

Acknowledgments

The present work has been performed in the scope of the activities of the AeroG-Aeronautics and Astronautics Center of the Portuguese Associate Laboratory in Energy, Transport and Aeronautics.

The financial support of the FCT-Fundação para a Ciência e Tecnologia of the Portuguese Ministry of

Science under Contract No. PTDC/EME/-MFE/ 102190/2008 is gratefully acknowledged.

References

[1] W. Bernhard, S. Sebastian, Multiple jet impingement: A review, Heat Transfer Research 42 (2) (5) (2011) 101-142.

[2] J.M.M. Barata, D.F.G. Durão, J.J. McGuirk, Numerical study of single impinging jets through a crossflow, Journal of Aircraft 26 (11) (1989) 1002-1008.

[3] J.M.M. Barata, Fountain flows produced by multiple impinging jets in a crossflow, AIAA Journal 34 (12) (1996) 2523-2530.

[4] F. Durst, A. Melling, J.H. Whitelaw, Principles and Practice of Laser-Doppler Anemometry, 2nd ed., New York, Academic Press, 1981.

[5] W.J. Yanta, R.A. Smith, Measurements of turbulent transport properties with a Laser-Doppler velocimeter, in: 11th Aerospace Sciences Meeting, Washington, 1978.

[6] A. Melling, J.H. Whitelaw, Turbulent flow in a rectangular duct, J. Fluid Mechanics 78 (1975) 285-315.

[7] C.J. Baker, The turbulent horseshoe vortex, Journal of Wind Engineering and Industrial Aerodynamics 6 (1981) 9.

[8] J. Andreopoulos, W. Rodi, Experimental investigation of jets in a crossflow, Journal of Fluid Mechanics 138 (1984) 127.

[9] M.J. Siclari, D. Migdal, T.W. Luzzi, J. Barche, J.L. Palcza, Development of theoretical models of jet-induced effects on V/STOL aircraft, Journal of Aircraft 13 (12) (1976) 938-944.

[10] D.R. Kotansky, The modeling and prediction of multiple VTOL aircraft flow fields in ground effect, AGARD CP-308 (1982) 16.